Q. J. R. Meteorol. Soc. (1990), **116,** pp. 989–1004 551.511.61:551.556.2:532.54

A perturbation analysis of turbulent flow through a porous barrier

By J. D. WILSON, G. E. SWATERS and F. USTINA
University of Alberta, Edmonton, Canada

(Received 13 April 1988; revised 13 November 1989)

SUMMARY

Earlier attempts to calculate the mean velocity field in flow about a thin, finite porous barrier (wall-mounted or otherwise) are reviewed. By simplifying the governing mean vorticity equation and expanding the flow variables in powers of the pressure-loss coefficient of the barrier (k_r) we derive an analytical solution for the mean velocity field in unbounded and homogeneous turbulent flow through a finite barrier. This solution is compared with the earlier solution of Kaiser (1959) and with numerical solutions for windbreak flow (bounded, inhomogeneous turbulence), and it is shown that all these solutions demonstrate a rate of recovery of the mean velocity field which is slower than is observed. It is suggested that the weakness of all the solutions lies in the treatment of the Reynolds stresses. A further point of interest is that a useful approximation to the pressure field may be obtained by dropping the Reynolds stress terms and solving a simplified equation expressing a balance between streamwise advection, pressure gradient, and localized momentum removal at the barrier; this might prove useful for the solution of more general porous barrier flows.

1. INTRODUCTION

This paper is concerned with calculation of turbulent flow through a porous barrier. The original hope was to obtain an analytical solution for windbreak flow, but we have succeeded only in the much simpler task of finding a perturbation solution for the passage of homogeneous turbulence through a finite porous barrier in a two-dimensional mean flow. We hope we will be forgiven for leading the reader (briefly) through a background survey and a derivation which are more general than is our solution, because although some may be interested in this simplest of all turbulent barrier flows—relating, for example, to the case of a long barrier (such as a bridge, perhaps) set well above ground—we expect our results will appeal also to those with a curiosity for the ability of the classical approach (analytical solution of the Reynolds equations with gradient-diffusion closure) to simulate the aerodynamics of windbreak flow.

Bradshaw (1973) stated that 'the most difficult flows to predict will be those in which a shear layer has its turbulence structure perturbed by a short region of strong pressure gradients and extra rates of strain, and then emerges into a longer region in which its Reynolds stress gradients are significant compared to smaller pressure gradients.' Windbreak flow is such a flow, and Counihan *et al.* (1974) noted that 'despite an enormous number of measurements of the wind behind full-scale and model fences and shelter belts, there are not even any useful empirical formulae[1] describing the sheltering effects of these obstructions'. Since the time of those contributions much has been learned from well-instrumented windbreak experiments (particularly Raine and Stevenson 1977, and Bradley and Mulhearn 1983) and there has been some progress in prediction. The most recent analytical contribution remains that of Counihan *et al.*, a perturbation solution for the velocity in the far wake of a solid barrier. Numerical integrations of the governing equations averaged over time or space, with various standard closure relationships, (Hagen *et al.* 1981; Wilson 1985) show promising comparison with observation, but are certainly in need of improvement.

[1] This was perhaps an overstatement since it had long been recognized that a porous fence is preferable to a solid one, and optimal ranges of porosity had been suggested.

If the barrier is sufficiently porous, the flow pattern can be only slightly different from the equilibrium (approach) flow: this suggests a perturbation analysis. In the following sections we review briefly the aerodynamics of windbreak flow, and survey past attempts to predict barrier flows. Thereafter we parametrize the momentum removal process in the governing equations, and perform a perturbation analysis, obtaining an exact solution for the 'bare bones' problem alluded to above and, for the windbreak case, a crude solution which at least estimates the magnitude of the velocity reduction.

In most cases symbols are defined in the text where they first appear. In addition, symbols, terminology, and notation are explained in an appendix.

2. Definition of the flow and survey of earlier work

(a) *Characterizing the approach flow and the barrier*

The simplest real windbreak flow is a neutrally-stratified atmospheric surface-layer (ASL) flow perpendicular to an infinitely long windbreak. The state of the undisturbed ASL will for present purposes be taken as controlled by the friction velocity u_* and the surface roughness length z_o alone. We will express the variation of the streamwise velocity with height in the undisturbed ASL using the power-law profile $\overline{u} = \overline{u}_H\,(z/H)^m$, where H is the fence height. This is a reasonable approximation to the (actual) logarithmic profile for heights larger than about $50z_o$, is analytically more tractable, and will permit a methodical simplification of the linearized governing equation. To ensure the shear stress is height-independent, instead of specifying the eddy viscosity (correctly) as $K = k_v u_* z$, we write $K = K_H(z/H)^n$, where $n = 1 - m$ for $m \neq 0$. With this choice for the undisturbed profiles of velocity and eddy viscosity the governing equation for the mean vorticity, which we derive later, can approximate either real windbreak flow (i.e. a wall-mounted barrier), in which case $m \sim 1/7$, or, with $m = n = 0$, the flow of homogeneous turbulence through a barrier. It is for the latter (free-slip) case that we have been able to obtain an exact solution.

A porous barrier is conveniently characterized by its 'pressure-loss' or 'resistance' coefficient, $k_r(\theta)$ (Laws and Livesey 1978). This is defined with reference to a calibration flow wherein the barrier is mounted so as to block a wind tunnel with the normal to the barrier inclined at angle θ to the stream. The resistance coefficient is formed by normalizing the pressure drop Δp across the barrier by ρu^2 (sometimes by $\rho u^2/2$), $k_r(\theta) = \Delta p/\rho u^2$. We will assume θ to be very small and write $k_r(0) = k_r$. Evidently, $k_r \rho u^2 = \Delta p$ is the force per unit area exerted by the barrier on the flow and vice versa. To a first approximation one might expect that in an unbounded flow through a porous barrier, provided the streamline inclination relative to the barrier is small, the primary effect of each element $\Delta y \Delta z$ of barrier area would be to exert a localized retarding force $F_D = k_r \rho u^2 \Delta y \Delta z$ on the airstream (where u is the streamwise velocity at the barrier element).

The resistance coefficient is easily measured, and may be correlated with the porosity and type of construction of the barrier (e.g., Baines and Peterson 1951). Being an aerodynamic rather than a geometric property, its use as a characterizing attribute is much preferable to the use of porosity. Flows through barriers of equal porosity and span may differ substantially but differences between flows through barriers of equal resistance coefficient and span, but unequal porosity, will be difficult to detect.

(b) *Overview of the aerodynamics of flow through a porous barrier*

An old review of many of the early measurements of windbreak flow is given by van Eimern *et al.* (1964). Heisler and DeWalle (1988) review the effect of windbreak structure

on wind flow and in the same book McNaughton (1988) reviews the windbreak effect on microclimate.

(i) *Mean velocity field.* Momentum is removed from the flow at the barrier. This causes a mean velocity deficit both downstream and (as a result of pressure effects) for a shorter range upstream. Immediately cross-stream from (above, in the windbreak case) the barrier there is a sharp and shallow zone of increased velocity so that

$$\int \bar{u}(z)\,dz = \int \bar{u}_o(z)\,dz = \text{constant} \tag{1}$$

where $\bar{u}_o(z)$ is the unperturbed approaching velocity profile and the integral spans the range of the cross-stream coordinate. Between the speed-up region and the velocity-deficit region is a region of very strong wind shear $\partial\bar{u}/\partial z$. The action of the shear stress $\overline{u'w'}$ (itself increased in this region) upon this shear converts mean kinetic energy to turbulent kinetic energy at an increased rate (relative to the undisturbed flow). The consequence is a spreading zone of increased turbulence (again relative to the undisturbed flow). The turbulent convection of mean momentum back from the speed-up region to the decelerated region causes recovery of the velocity field.

(ii) *Turbulent velocity field.* Formally, i.e. in the conservation equations, the flow interaction with the barrier may be treated by adopting a spatial averaging procedure (see Wilson and Shaw 1977; Raupach and Shaw 1982; Finnigan 1985), and as a result of the spatial averaging there appear terms which may be identified with the viscous and form drag. The (fluctuating) drag converts mean kinetic energy (MKE) to turbulent kinetic energy (TKE) at the barrier, and also exerts a drag on the turbulent flow, passing energy from larger eddies to smaller eddies on the scale of the barrier elements. In spite of this strong production of TKE at the barrier, observations (Raine and Stevenson 1977; Wilson 1987) show a zone of reduced TKE in the near lee of a porous barrier, bounded by the spreading wake of increased TKE generated by the increased shear production in the strong-shear zone. Presumably the very small scales of motion being fed with energy at the barrier are subject to very rapid dissipation.

(c) *Prediction of porous barrier flow*

G. I. Taylor (1944) gave a solution for the velocity perturbation upstream of a finite or infinite porous plate perpendicular to an unbounded laminar flow. Taylor hypothesized that the effect of each area element $\Delta y\Delta z$ of the barrier on the flow upstream of the barrier is equivalent to the effect of a source of fluid volume of strength $k_r\,u\,\Delta y\Delta z$ placed at the same point. For small k_r Taylor's result for the velocity immediately upstream of a finite barrier is $u/u_o = 1-k_r/2$. Our solutions confirm this result (see Fig. 2), and several authors, including Graham (1976), have shown agreement between experiment and Taylor's theory.

De Bray (1971) was concerned with the design of practical windbreaks (i.e. wall-mounted barriers in turbulent shear flow) but apparently applied Taylor's methodology to obtain a prediction of the leeward velocity. It is not clear how Taylor's result can be extended to predict the leeward flow, and the argument is not given, but de Bray's result for the leeward velocity is, for small k_r, $u/u_o = 1-k_r$. It will be seen later that this (not very accurate) result follows from neglect of the Reynolds stress terms in the governing equations.

Tani (1958) and Kaiser (1959) treated the windbreak as a source of momentum-deficit and adopted a passive scalar diffusion model (essentially the Gaussian plume model) for the spread of this deficit. That this approach is seriously deficient may be

shown by substituting into the governing mean streamwise momentum-equation the expansion

$$\bar{u} = \bar{u}_o + k_r \Delta\bar{u} \qquad \bar{w} = k_r \Delta\bar{w} \qquad \bar{p} = k_r \Delta\bar{p}$$

where $\Delta\bar{u}$, $\Delta\bar{w}$ are the velocity disturbances and $\Delta\bar{p}$ is the pressure disturbance. One obtains, to first order in k_r,

$$\bar{u}_o \frac{\partial \Delta\bar{u}}{\partial x} + \Delta\bar{w} \frac{\partial \bar{u}_o}{\partial z} = -\frac{1}{\rho} \frac{\partial \Delta\bar{p}}{\partial x} + K \frac{\partial^2 \Delta\bar{u}}{\partial z^2} \tag{2}$$

where the term $\partial\overline{u'^2}/\partial x$ has been dropped and first-order closure (with constant K) has been adopted to parametrize $\partial\overline{u'w'}/\partial z$. But the Gaussian plume model is the solution to the much simpler advection-diffusion equation,

$$u_o \frac{\partial \Delta\bar{u}}{\partial x} = K_o \frac{\partial^2 \Delta\bar{u}}{\partial z^2} \tag{3}$$

(where both u_o and K_o are constants). Tani and Kaiser have in effect neglected the pressure gradient, permitted free slip along the wall (no momentum flux to ground), and adopted a spatially-constant eddy viscosity to parametrize the momentum flux. Furthermore the source of momentum excess which would be needed to satisfy the integral constraint (Eq. 1) on the horizontal flux of air mass is not included and the momentum sink strength is evaluated using the unperturbed velocity field, whereas the actual velocity at the fence is reduced (according to Taylor's findings, by an amount of order $k_r u_o/2$ for small k_r). Despite these limitations, the Tani–Kaiser approach does predict a wind reduction of the correct order of magnitude for small k_r. Kaiser gave solutions both for a single momentum sink of strength $Q = k_r \rho u_o^2 H$ placed at $z = H$ and for a collection of strip sources of width dz and strength $dQ = k_r \rho u_o^2 dz$ extending to $z = H$. The latter solution is

$$\frac{1}{k_r} \frac{\Delta\bar{u}}{u_o} = -1/2 \left\{ \operatorname{erf}\left(\frac{1+z}{2\sqrt{(x/R)}} \right) + \operatorname{erf}\left(\frac{1-z}{2\sqrt{(x/R)}} \right) \right\} \tag{4}$$

where x, z are dimensionless (scaled on H) and $R = u_o H/K_o$. This is shown on Fig. 2 in comparison with our solutions; the location of the velocity minimum is poorly predicted owing to the neglect of the pressure gradient.

Plate (1971) noted that observations of the mean wind profile in the lee of sharp-edged solid barriers reveal a region of very strong vertical shear (lying at $z \sim H$ for small x), separating the region of reduced mean velocity near the ground from a region of increased mean velocity aloft. Recognizing the oversimplification involved, Plate identified an 'intrinsic' streamwise coordinate lying in this strong-shear region, and considered this as an axis separating two slabs of air whose interaction he represented as that of an upper stream of initially (i.e. at $x = 0$) uniform velocity U_2 interacting via turbulent momentum exchange with a lower stream of (again initially) uniform velocity U_1. Assuming the eddy viscosity to vary as $K = x(U_2 - U_1)/(4\sigma^2)$, one obtains a standard mixing-layer solution involving the empirical parameter σ. With the choice $\sigma \sim 15$, observations of the velocity profile in the strong-shear region behind solid barriers were shown to be in good agreement with the solution; but it is probably the use of an x-dependent eddy-viscosity, becoming large at large x, and the flexibility afforded through σ which allow Plate's solutions to match observation.

Counihan *et al.* (1974) presented an analytical theory for the mean velocity field in the far ($x/H \geq 10$) wake of solid obstacles in a turbulent wall-layer of depth δ (with

obstacle height $H \ll \delta$). The restriction to the far wake is a consequence of the fact that the flow perturbation due to a solid obstacle can never be small near the obstacle. One of the interesting findings is that the leeward fractional velocity change $\Delta\overline{u}/\overline{u}_o$ is approximately height-independent in the lower 'wall region' of the wake: this is also the case behind porous barriers. Bradley and Mulhearn (1983) presented measurements which supported the theory in its prediction of the shapes of the far-wake velocity and shear-stress profiles and of the rate of decay of the velocity perturbation: the theory underestimated the magnitude of the stress perturbation.

Turning now to numerical studies, Counihan *et al.* stated that 'it would be interesting to see the computational methods for solving elliptic problems . . . (recently developed) . . . being applied to the (surface obstacle) problem.' Several years later, Durst and Rastogi (1980) reported numerical simulations and wind-tunnel measurements of flow about wall-mounted solid barriers. These authors used the '$k-\varepsilon$' turbulence model, a first-order closure scheme in which the local eddy viscosity K is formed from the local turbulent kinetic energy k and its dissipation rate ε, for which approximate budget equations are included (see Launder and Spalding 1974). The length of the leeward re-circulation zone was predicted fairly successfully, provided a very fine grid resolution was employed: the need for high resolution in modelling is not surprising in view of the no-slip condition and associated boundary layers on a solid obstacle.

Hagen *et al.* (1981) applied the '$k-\varepsilon$' model to flow about porous fences, but incorporated the effect of the fence by imposing a velocity profile (in effect an extra boundary condition) in the very near lee of the fence (as well as far upstream). Wilson (1985) instead parametrized the porous barrier as a localized momentum sink of strength $k_r\rho\,\overline{u}\,|\overline{u}|$ (where $\overline{u}$ is the local mean velocity) in the governing mean-streamwise momentum equation. As argued earlier, this is a reasonable first approximation for the effect of the fence, provided the streamline inclination is not large. By comparing simulations with the experimental data of Bradley and Mulhearn (1983), Wilson showed that good predictions of the depth of the near-lee velocity minimum are obtained with modest computational effort (i.e., a fairly coarse grid), with no calibration (i.e., a standard numerical scheme and closure hypothesis and with all inputs z_o, H, k_r specified in the experimental data), and regardless of whether one adopted the simplest conceivable closure scheme ($K(x,z) = K_o(z) = k_v u_{*o} z$, where u_{*o} is the far upstream friction velocity), the more complex '$k-\varepsilon$' model, or a full second-order closure scheme. The numerical solutions, regardless of closure scheme, did not predict the sharp and shallow speed-up zone observed above the fence and underestimated the rate of recovery of the velocity field (the latter deficiency being at least partly a consequence of the former). The similarity in this respect of the analytical solution derived here suggests that the weakness of the numerical solutions stems from inadequacy of the closure scheme(s) rather than from numerical limitations such as grid resolution.

3. Governing equations and perturbation expansion

(*a*) *Governing equations*

The presence of a porous barrier means that the Navier–Stokes equations must in principle be solved subject to the no-slip condition on a surface having very complex geometry. An alternative (see Fig. 1) is to consider the barrier as splitting the region $z<H$ into an upstream region $x<-l/2$ and a downstream region $x>l/2$ (where l is the thickness of the barrier). One must now relate the velocity and pressure along the upwind face $x = l/2$ of the downstream region to the pressure and velocity at $x = -l/2$, the exit face of the upstream region: conservation of mass requires $U_L = U_R = U_B$ (where U_B is

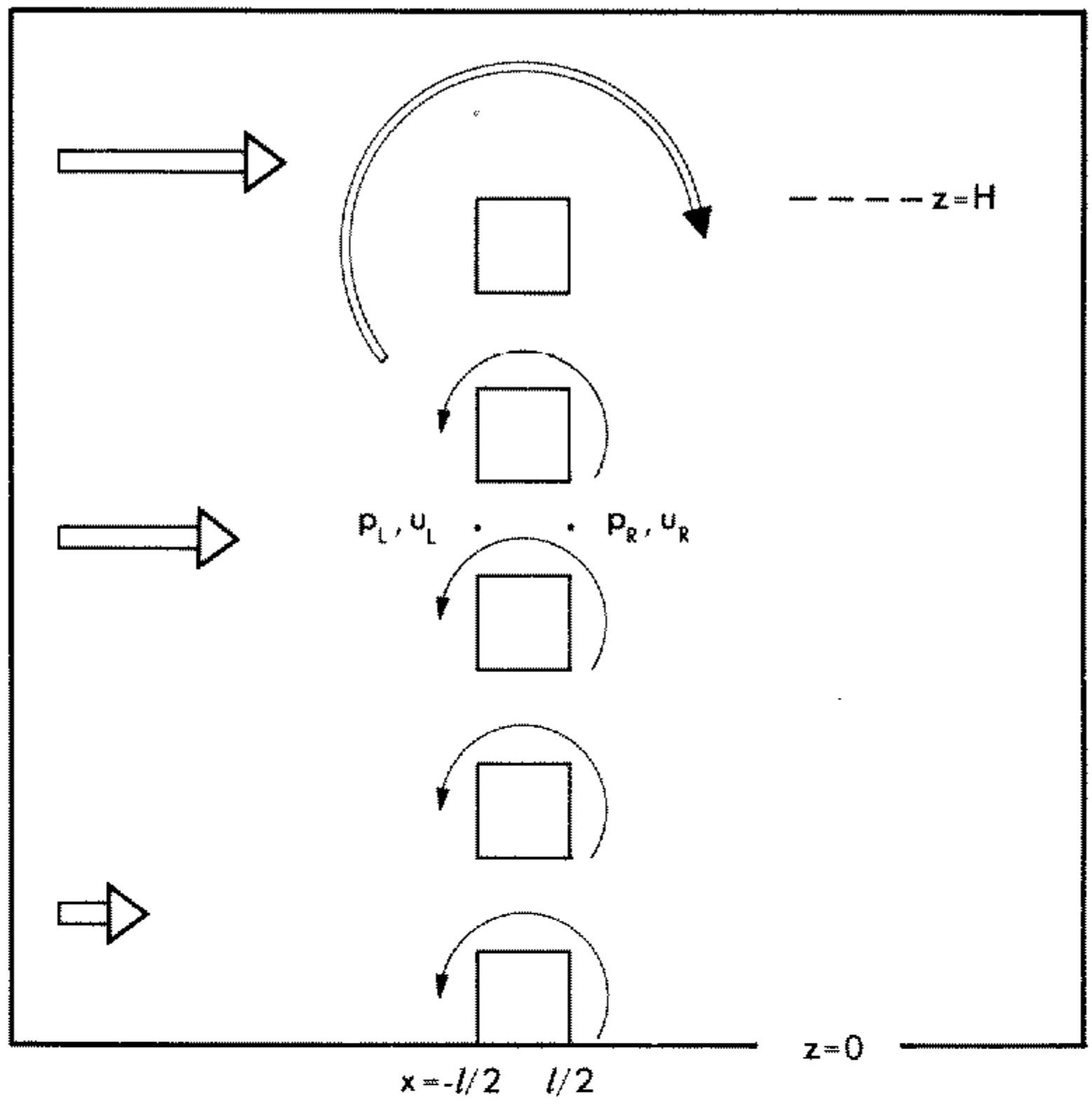

Figure 1. Illustrating that the porous barrier splits the region $0 \leq z \leq H$ into an upwind and a downwind region separated by an excluded region $-1/2 \leq x \leq 1/2$. The pressures and streamwise velocities on the boundaries of the excluded region are linked by the equations $u_L = u_R = u$ (a requirement of mass conservation) and $p_L - p_R = k_r \rho u^2$, where k_r is the resistance coefficient of the barrier. Also shown, with circular arrows, are the regions (and associated signs) of vorticity production. The dominant effect of the barrier is to cause vorticity production at the tip of the barrier (double circular arrow). Shear in the approaching flow (illustrated by the horizontal double arrows) results in vorticity production of opposite sign distributed along the barrier.

the velocity 'at' the barrier—actually an average across a frontal area large with respect to the area of the pores in the barrier since the flow 'at' the barrier will be organized into jets), and the pressure difference is given by $P_L - P_R = \Delta p = \rho k_r u|u|$. The vertical and lateral velocities are not necessarily continuous across the barrier (the angle of exit from the barrier need not equal the angle of entry), but these (small) effects will be neglected.

With this divided domain, the pressure gradient $(\partial p/\partial x)_{x=0}$ is meaningless (below $z = H$) because $x = 0$ is excluded; but we will nevertheless adopt as valid at all points the equations

$$\frac{\partial u}{\partial t} + u_j \frac{\partial u}{\partial x_j} = -\frac{1}{\rho}\frac{\partial p}{\partial x} + \nu \nabla^2 u - k_r u|u|\, \delta(x,0) s(z,H) \tag{5a}$$

$$\frac{\partial w}{\partial t} + u_j \frac{\partial w}{\partial x_j} = -\frac{1}{\rho}\frac{\partial p}{\partial z} - g + \nu \nabla^2 w \tag{5b}$$

where

$$s(z,H) = 1 \quad \text{for } z \leqslant H \qquad s(z,H) = 0 \quad \text{for } z > H.$$

Equation (5a) is valid at $x = 0$ in the sense that when integrated throughout a region $-l/2 \leq x \leq l/2$ it yields the correct pressure drop $\Delta p = k_r \rho\, u\,|u|$. When integrated through-

out a larger control volume spanning $x = 0$ (as, for example, is the time-average streamwise equation in the numerical model of Wilson (1985)) the streamwise entry and exit velocities on the control volume faces differ and the pressure difference across the control volume no longer solely balances the drag on the barrier.

Now let us time-average Eqs. (5) in the normal way. Restricting to two-dimensional mean flow perpendicular to an infinitely-long barrier, defining $\bar{p}$ to be the mean departure from a hydrostatic state, and neglecting viscous momentum fluxes, we obtain

$$\bar{u}\frac{\partial \bar{u}}{\partial x} + \bar{w}\frac{\partial \bar{u}}{\partial z} = -\frac{1}{\rho}\frac{\partial \bar{p}}{\partial x} - \frac{\partial \overline{u'w'}}{\partial z} - \frac{\partial \overline{u'^2}}{\partial x} - k_r \overline{u|u|}\,\delta(x,0)s(z,H) \tag{6a}$$

$$\bar{u}\frac{\partial \bar{w}}{\partial x} + \bar{w}\frac{\partial \bar{w}}{\partial z} = -\frac{1}{\rho}\frac{\partial \bar{p}}{\partial z} - \frac{\partial \overline{u'w'}}{\partial x} - \frac{\partial \overline{w'^2}}{\partial z}. \tag{6b}$$

If we assume that $u(t)$ is at all times positive (which will nearly always be true except very near the ground), then $\overline{u|u|} = \overline{u^2} = \bar{u}^2 + \overline{u'^2}$. In the atmospheric surface layer, not too close to the ground, one may neglect $\overline{u'^2}$ relative to $\bar{u}^2$; we will assume this to be generally permissible. Hence, the streamwise momentum equation employed here is the usual time-average equation with an added term $-k_r\bar{u}^2$ at the barrier accounting for loss of momentum to the barrier; each elementary area $\Delta y \Delta z$ of the barrier exerts a time-average force in the negative x-direction of $k_r\rho\,\bar{u}^2\Delta y\Delta z$.

We can expect analytical solutions to Eqs. (6) to yield a discontinuity in pressure at $x = 0$, $z < H$. If the pressure field is known at all x and correspondingly imposed, there is no need to retain the momentum sink in Eq. (6a), whose inclusion is necessary only to generate the required pressure discontinuity (this approach is taken in the approximate solution of section 4(b)).

Because the mean flow under consideration is two-dimensional, the mean vorticity has only one component, $\Omega = \partial\bar{u}/\partial z - \partial\bar{w}/\partial x$. The governing equation for Ω is readily derived by differentiating Eqs. (6) to obtain

$$\bar{u}\frac{\partial \Omega}{\partial x} + \bar{w}\frac{\partial \Omega}{\partial z} = -\frac{\partial^2 \overline{u'w'}}{\partial z^2} + \frac{\partial^2 \overline{u'w'}}{\partial x^2} + \frac{\partial^2}{\partial x \partial z}(\overline{w'^2} - \overline{u'^2}) + \\ + k_r\bar{u}^2\delta(x,0)\delta(z,H) - k_r\delta(x,0)s(z,H)\partial\bar{u}^2/\partial z. \tag{7}$$

As indicated in Fig. 1, the first term on the right-hand side represents a source of positive vorticity at the tip of the barrier, while the second term, which will usually be of lesser importance, represents a distributed source of negative vorticity along the barrier at $z < H$. Dr. J. J. Finnigan (personal communication) has suggested that retention of this second term might be inconsistent with neglecting the possible change in flow direction across the barrier.

In the subsequent analysis the term

$$\frac{\partial^2}{\partial x \partial z}(\overline{w'^2} - \overline{u'^2})$$

in the vorticity equation will be neglected. This is probably not a serious simplification as the simulations of Wilson (1985) indicate that gradients in $\overline{u'^2}$ and $\overline{w'^2}$ play only a small part in the momentum balance of a shelter flow. The shear stress $\overline{u'w'}$ will be modelled using first-order closure, $\overline{u'w'} = -K\partial\bar{u}/\partial z$, with the eddy viscosity K treated as unaffected by the flow perturbation due to the windbreak, i.e. K independent of the streamwise coordinate. This is a radical simplification, yet Wilson (1985) found that such an assumption yields predictions of the flow reduction in the near lee of a 50% porous windbreak (having $k_r = 2$) which are almost as good as those resulting from more complex

first-order closure schemes, (e.g. '$k-\varepsilon$') and from use of a Reynolds stress model (wherein simplified budget equations for the shear stress, the velocity variances, and the TKE dissipation rate are included). Presumably therefore, when $k_r \ll 1$ (the intended case here) the assumption of an unperturbed eddy-viscosity profile is not much worse than the adoption of any of the closure schemes available at present.

Let us define a mean streamfunction Φ such that

$$\overline{u} = -\Phi_z \qquad \overline{w} = \Phi_x \qquad \nabla^2\Phi = -\Omega. \tag{8}$$

Substituting the streamfunction into the vorticity Eq. (7) and multiplying through by $(H/\overline{u}_{oH})^2$, one obtains the dimensionless vorticity equation

$$\Phi_z(\Phi_{xxx} + \Phi_{xzz}) - \Phi_x(\Phi_{xxz} + \Phi_{zzz}) = -\left(\frac{1}{R}\right)\left\{\frac{\partial^2}{\partial z^2}(z^n\Phi_{zz}) - \frac{\partial^2}{\partial x^2}(z^n\Phi_{zz})\right\} +$$

$$+ k_r\Phi_z^2\delta(x,0)\delta(z,1) - 2k_r\delta(x,0)\mathrm{s}(z,1)\Phi_z\Phi_{zz}. \tag{9}$$

where all lengths are now scaled by H, all velocities by $\overline{u}_{oH}$ (the dimensionless velocities will be denoted in roman type $\mathrm{u} = \overline{u}/\overline{u}_{oH}$, $\mathrm{w} = \overline{w}/\overline{u}_{oH}$), and $R = \overline{u}_{oH}H/K_H$ is a Reynolds number based on the turbulent viscosity. Specifying $K_H = k_v u_* z$ and $\overline{u}_{oH} = (u_*/k_v)\ln(H/z_o)$, we obtain $R = 38 \gg 1$ for the case $H/z_o = 500$.

(b) *Perturbation expansion*

Now let us expand the streamfunction in powers of the (small) resistance coefficient,

$$\Phi = \phi_o + k_r\phi^{(1)} + k_r^2\phi^{(2)} + \ldots \tag{10}$$

where the unperturbed streamfunction is $\phi_o = -z^{1+m}/(1+m)$. The corresponding expansions for the dimensionless velocities are $\mathrm{u} = \mathrm{u}_o + k_r\mathrm{u}^{(1)} + \ldots$, $\mathrm{w} = k_r\mathrm{w}^{(1)} + \ldots$ and to first-order in k_r we have $\Delta\overline{u}/\overline{u}_{oH} = k_r\mathrm{u}^{(1)}$. If earlier suggestions as to the magnitude of $\Delta\overline{u}$ in the near lee of the barrier are correct, we may expect to find $\mathrm{u}^{(1)} \sim -1$ in that region.

Substituting the expanded stream-function into Eq. (9) and collecting the coefficients of k_r^1 we obtain the governing equation for the lowest-order perturbation to the stream-function $\phi^{(1)}$

$$\nabla^2\phi_x^{(1)} + \{(m - m^2)/z^2\}\phi_x^{(1)} = \left(\frac{1}{R}\right)z^{-m}\left\{\frac{\delta^2}{\partial z^2}(z^n\phi_{zz}^{(1)}) - \frac{\partial^2}{\partial x^2}(z^n\phi_{zz}^{(1)})\right\} -$$

$$-z^m\delta(x,0)\delta(z,1) + 2mz^{m-1}\delta(x,0)\mathrm{s}(z,1). \tag{11}$$

In section 4 we give a solution to Eq. (11) for the case $m = 0$, and in section 5 we examine the predicted velocity reduction when approach shear is included by neglecting the term in $(1/R)$ and further expanding $\phi^{(1)}$ in m.

4. FREE SLIP SOLUTIONS

As stated at the outset, we have been unable to solve the vorticity equation for a wall-mounted barrier, even in the simplified form of Eq. (11). Here, setting $m = n = 0$, we focus on the simplest member of the class of turbulent streams disturbed by a porous barrier. There is no shear in the approach flow and the turbulence is homogeneous. Physically, the simplified equation represents one or other of the (equivalent) problems:

(i) An unbounded flow through a barrier of extent $-H \leq z \leq H$, with symmetry about $z = 0$, at which plane $\overline{w} = 0$ and $\partial\overline{u}/\partial z = 0$.

(ii) Flow bounded at $z = 0$ by a wall along which free slip is permitted.

A flow of this type may be realized by, for example, forcing a porous but rigid net to move through a fluid which is in homogeneous turbulent motion.

We will give an exact solution, then show that by neglecting the turbulent diffusion terms one may obtain a simple expression for the pressure field which, when *imposed* in the streamwise momentum equation, results in a solution almost the same as the exact solution.

(*a*) *Exact solution*

For clarity the superscript on the perturbation streamfunction will be dropped. With $m = n = 0$ Eq. (11) reduces to

$$\nabla^2 \phi_x + \frac{1}{R}[\phi_{xxzz} - \phi_{zzzz}] = -\delta(x,0)\delta(z,1) \tag{12}$$

and we will impose boundary conditions:

$$\begin{aligned} &\phi \to 0 \quad \text{as } |x| \to \infty \\ &\phi \to 0 \quad \text{as } z \to \infty \\ &\phi = \phi_x = \phi_{zz} = 0 \quad \text{at } z = 0. \end{aligned} \tag{13}$$

To progress, we replace the boundary condition at $z = \infty$ with the same condition at an arbitrary location $z = L$. Then if we write

$$\phi = \sum_{n=1}^{\infty} X^n(x)\sin(n\pi z/L) \tag{14}$$

the conditions at $z = 0$ and $z = L$ are automatically satisfied. Substituting this decomposition into Eq. (12), multiplying throughout by $\sin(m\pi z/L)$, and integrating from $z = 0$ to $z = L$, we obtain an ordinary differential equation for the X^n,

$$X^n_{xxx} - a_n X^n_x - (a_n/R)X^n_{xx} - (a_n^2/R)X^n = -(2/L)\delta(x,0)\sin(n\pi/L) \tag{15}$$

where $a_n = (n\pi/L)^2$. Since ϕ (and therefore X^n) must vanish at $|x| = \infty$, we may take the Fourier transform of Eq. (15). Defining the transform of $X^n(x)$ by

$$\hat{X}^n(k) = \int_{-\infty}^{\infty} X^n(x)\exp(-\mathrm{i}kx)\, dx \tag{16}$$

where $\mathrm{i} = \sqrt{(-1)}$ and k is the wavenumber, we obtain the equation

$$\hat{X}^n(k) = \{(2/L)\sin(n\pi/L)\}/B(k) \tag{17}$$

where

$$B(k) = \mathrm{i}k^3 + \mathrm{i}ka_n - (a_n/R)k^2 + (a_n^2/R). \tag{18}$$

The equation $B(k) = 0$ has three imaginary roots $k_j = \mathrm{i}k_{*j}$ (k_{*j} real), two of which are positive and one negative. To invert Eq. (17) we write

$$X^n(x) = \frac{1}{2\pi}\int_{-\infty}^{\infty} \hat{X}^n(k)\exp(\mathrm{i}kx)\, dk = \{\sin(n\pi/L)/(\pi L)\} \oint \{\exp(\mathrm{i}kx)/B(k)\}dk \tag{20}$$

where the return contour linking $k = \infty$ and $k = -\infty$ will be chosen to lie at $|k| = \infty$ in such a way that $\exp(\mathrm{i}kx)$ vanishes. By the residue theorem (Churchill *et al.* 1974) we may write

$$X^n(x) = (2\mathrm{i}/L)\sin(n\pi/L) \sum_j R_j \tag{21}$$

where the R_j are the residues of $\exp(ikx)/B(k)$ at the simple poles enclosed by the contour. In the present case, for a pole at $k = k_j$, we have

$$R_j = \exp(ik_j x)/B'(k_j) \tag{22}$$

where

$$B'(k_j) = \left(\frac{\partial B(k)}{\partial k}\right)_{k=k_j} = i\{-3k_{*j}^2 - (2a_n/R)k_{*j} + a_n\}. \tag{23}$$

Then

$$X^n(x) = (2/L)\sin(n\pi/L) \sum_{\substack{\text{enclosed}\\ \text{poles}}} \left(\frac{|k_{*j}|}{k_{*j}}\right) \frac{\exp(-k_{*j}x)}{a_n - 3k_{*j}^2 - 2(a_n/R)k_{*j}}. \tag{24}$$

This solution for the lowest-order perturbation streamfunction has been used to calculate the streamwise velocity perturbation $u^{(1)}$ and is shown on Fig. 2 for the case $H/z_o = 500$. The fractional velocity reduction in the near lee is of order k_r and minimum velocity occurs downstream from the barrier (because of the adverse pressure gradient at $x > 0$). Anyone familiar with the typical leeward extent of wind reduction behind a shelterbelt may find the very slow recovery exhibited by our solution to be surprising and, perhaps, unrealistic. We delay comment on this until section 6.

(*b*) *An approximate solution*

Equation (12) contains the small parameter $1/R$, and prior to obtaining the exact solution given above we carried out a further (singular) perturbation expansion in $1/R$ ('singular' because $1/R$ multiplies the terms of highest order, so the simplified equations

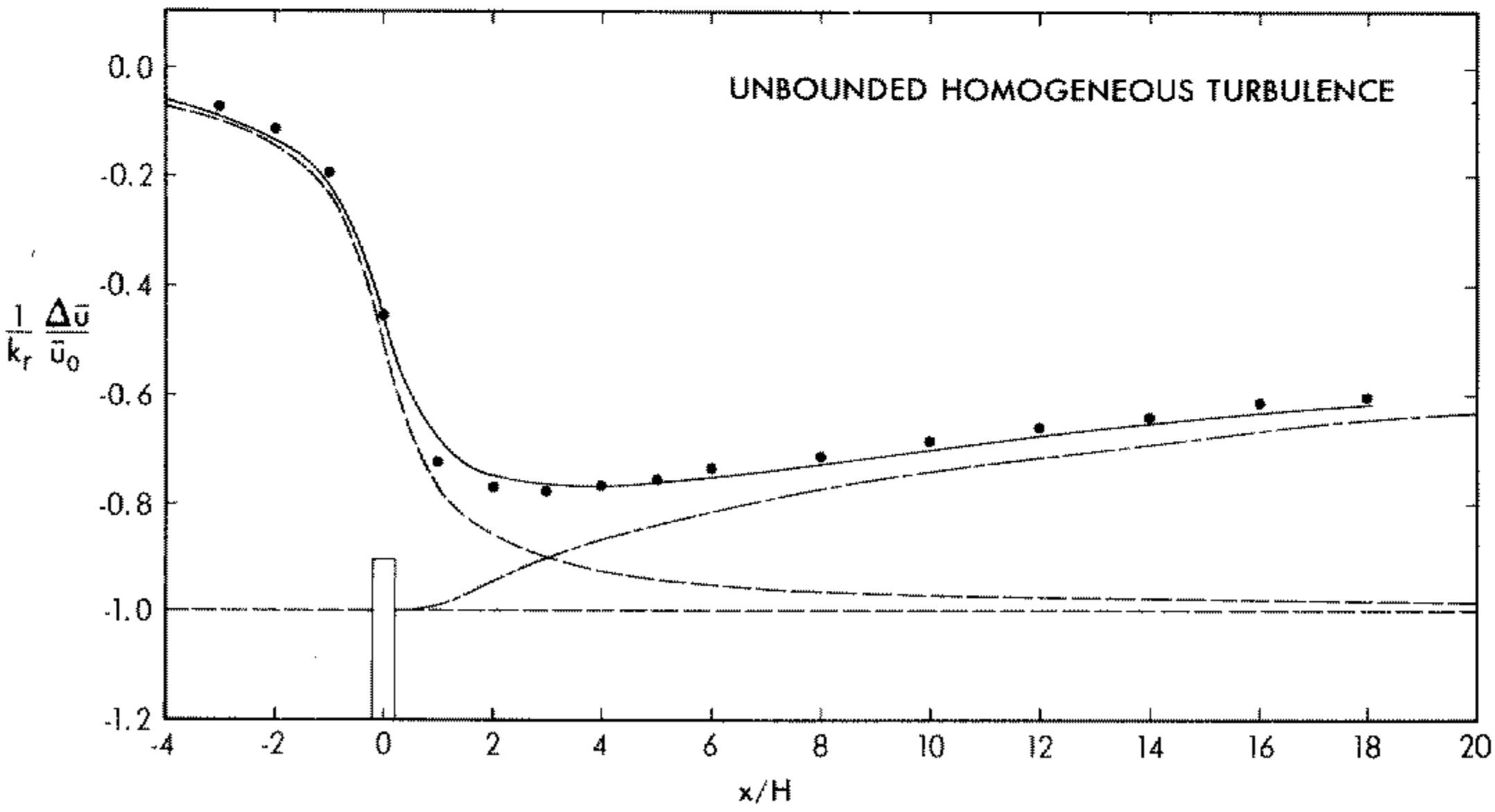

Figure 2. Analytical solutions for the fractional velocity change $(1/k_r)(\Delta\bar{u}/\bar{u}_o)$ as a function of streamwise location x/H at height $z/H = 1/2$, with $H/z_o = 500$. (i) The exact solution to first order in k_r, $u^{(1)}$, with $L = 80$ (——). (ii) Kaiser's solution, Eq. (4) (— — — —). (iii) The 'no diffusion' solution, Eq. (27) (– – – –) (iv) Approximate solution obtained by solving Eq. (30) using the Green's function method (Eqs. (31), (32)) for $x > -10$ with $u^{(1)}(-10,z) = 0$ and the pressure field p^* of equation (29); (●).

resulting from the expansion in $1/R$ cannot satisfy all the original boundary conditions.) The lowest-order term in the (now double) perturbation expansion is governed by

$$\nabla^2 \phi_x^* = -\delta(x,0)\delta(z,l) \tag{25}$$

where the superscript (*) denotes the solution to first order in k_r and to zeroth order in $(1/R)$. Using the appropriate Green's function (to enforce $w^* = 0$ along $z = 0$) one obtains as the solution to this Poisson equation

$$w^* = \frac{-1}{4\pi} \ln \frac{x^2 + (z-1)^2}{x^2 + (z+1)^2} \tag{26}$$

and with manipulation involving the continuity equation one obtains

$$u^* = \frac{1}{2\pi} \operatorname*{Lim}_{x_o \to -\infty} \left\{ \tan^{-1}\left(\frac{x}{z-1}\right) - \tan^{-1}\left(\frac{x_o}{z-1}\right) - \tan^{-1}\left(\frac{x}{z+1}\right) + \tan^{-1}\left(\frac{x_o}{z+1}\right) \right\} \tag{27}$$

This ('no diffusion') solution for the lowest-order perturbation is shown on Fig. (2). From upstream to a distance of about $x = 1$ downstream this solution differs little from the exact solution; however the velocity does not recover downstream because the turbulent momentum-transfer term which causes re-acceleration has been dropped. This grossly deficient solution is of little value, but there is an interesting aspect to it.

Let $p = \bar{p}/\rho \bar{u}_{oH}^2$ be the dimensionless pressure. The pressure field p^* corresponding to this 'no diffusion' velocity perturbation is governed by the equation

$$\nabla^2 p^* = -s(z,1)\delta_x(x,0) \tag{28}$$

where δ_x is the *derivative* of the delta function. The boundary condition along $z = 0$ is $p_z^* = 0$. The solution is

$$p^* = \frac{-1}{2\pi} \left\{ \tan^{-1}\left(\frac{1+z}{x}\right) + \tan^{-1}\left(\frac{1-z}{x}\right) \right\}. \tag{29}$$

The first-order pressure field is discontinuous at $x = 0$, $z < 0$ with

$$\operatorname*{Lim}_{\substack{x \to 0^- \\ z<1}} p^* = 1/2 \qquad \text{and} \qquad \operatorname*{Lim}_{\substack{x \to 0^+ \\ z<1}} p^* = -1/2,$$

i.e. the pressure drop across the fence, $\Delta \bar{p}$, is given by $-\rho k_r \bar{u}_o^2$ as expected.

We will now impose this perturbation pressure field in the equation

$$\frac{\partial u^{(1)}}{\partial x} = -\frac{\partial p}{\partial x} + \frac{1}{R} \frac{\partial^2 u^{(1)}}{\partial z^2} \tag{30}$$

which is the form of the $\bar{u}$-momentum equation corresponding to the simplified vorticity equation (12).

The solution to Eq. (30) may be obtained by the Green's function method: specifying the solution at an 'upstream' point x_l one has

$$u^{(1)}(x,z) = \int_{x'=x_l}^{x} \int_{z'=0}^{\infty} G(x,z;x',z')(-\partial p(x',z')/\partial x')\, dx'dz' + \int_{z'=0}^{\infty} G(x,z;x_l,z') u^{(1)}(x_l,z')\, dz' \tag{31}$$

where the appropriate Green's function is

$$G(x,z;x',z') = \frac{1}{\sqrt{\{4(x-x')/R\}}}\left\{\exp\left(\frac{-(z-z')^2}{4(x-x')/R}\right) + \exp\left(\frac{-(z+z')^2}{4(x-x')/R}\right)\right\} \quad (32)$$

The Kaiser solution shown on Fig. 2, (Eq. (4), given earlier), is easily obtained from Eqs. (31, 32) by choosing $x_l = 0$, $u^{(1)}(0,z') = -s(z',1)$, and setting the pressure gradient to zero in Eq. (31).

Now if we write $u^{(1)} = 0$ at $x_l = -10$ and specify the pressure field as p^* given in Eq. (29), we obtain a solution (see Fig. (2)) which is virtually the same as the exact solution to Eq. (12). The interesting question is the extent to which this finding might be generalized: may one, in a more complex barrier flow, facilitate a solution by first neglecting the stress gradients and obtaining an approximation to the pressure field which can subsequently be imposed in the full equation? Such a procedure would (superficially) resemble the practice of solving disturbed boundary-layer flows by calculating an outer-layer pressure perturbation and imposing this on the more complex inner layer.

5. Velocity reduction with approach shear

When the no-slip condition is retained we may further expand in the small parameter m (=1/7) the component of the streamfunction appearing at first order in k_r,

$$\phi^{(1)} = \phi^{(1)(0)} + m\phi^{(1)(1)} + \ldots.$$

We will examine only the 'no diffusion' solution. Substitution into Eq. (11) yields, dropping terms in $(1/R)$,

$$\nabla^2\phi_x^{(1)(0)} = -\delta(x,0)\delta(z,1) \quad (33)$$

$$\nabla^2\phi_x^{(1)(1)} = -\phi_x^{(1)(0)}/z^2 + 2z^{m-1}\delta(x,0)s(z,1). \quad (34)$$

The solution to Eq. (33) has already been given, and Eq. (34) is easily solved by the Green's function method (again we form the Green's function so as to ensure that the vertical velocity vanishes on $z = 0$). The solution confirms that

$$\lim_{x\to\infty}(1/k_r)(\Delta\bar{u}/\bar{u}_o) \approx -1$$

for heights near the ground, i.e. in the case of a wall-mounted barrier one may expect that the fractional velocity reduction in the near lee is approximately height-independent and has magnitude $\sim k_r$.

6. Discussion and conclusion

The analytical solutions give a rate of recovery of the velocity field which is much slower than one expects on the basis of observations behind barriers in the neutrally-stratified atmospheric surface layer, and it is of interest that numerical solutions (Wilson 1985) for windbreak flow likewise underestimate the rate of recovery. Figure 3 shows solutions (using second-order closure: methodology as described by Wilson 1985) for a fence in the neutral surface layer with $H/z_o = 600$ and $k_r = 0{\cdot}05$ and $2{\cdot}0$. The points to be noted are:

(i) As in our free-slip solution and the no-diffusion solution for small m, in the near lee, $(1/k_r)(\Delta\bar{u}/\bar{u}_o) \sim -1$ for small k_r.

(ii) For larger k_r the fractional velocity change is not as large as k_r and the rate of recovery is faster in the sense that, far from the fence (say at $x = 20$), the fractional velocity

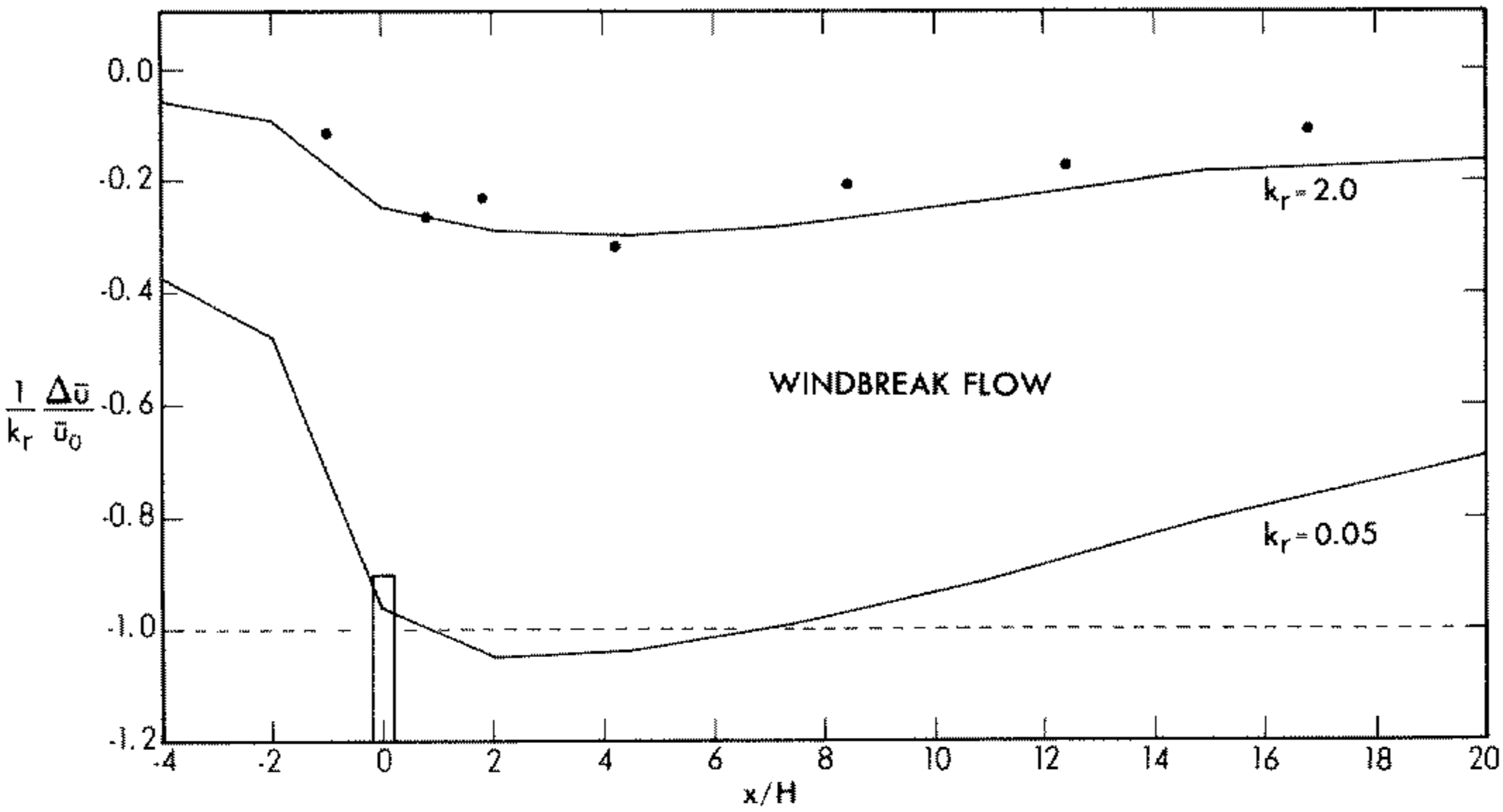

Figure 3. Numerical solutions for windbreak flow using second-order closure for the fractional velocity change at height $z/H = 0{\cdot}38$ for small and moderate values of the resistance coefficient k_r. The simulations were performed with $H/z_o = 600$, corresponding to the experiment of Bradley and Mulhearn (1983). Experimental data (for $k_r = 2$) is plotted (•).

reduction is a smaller proportion of its maximum (near-lee) value than is the case for small k_r.

It may be that observations behind very porous fences would confirm this slow recovery (the experimental difficulty of such an experiment is obvious—one is faced with accurately measuring very small mean velocity differences). On the other hand, even at large k_r, the numerical model underestimates the rate of recovery. Therefore we suspect that both the analytical solution for the free-slip flow and the (much more complex) numerical model for windbreak flow are deficient. Furthermore, the deficiency probably lies in the treatment of Reynolds stress because, having examined both analytical and numerical solutions, we can discount both numerical limitations (e.g. grid resolution) and the approximations of the analytical solution (linearization of advection by the mean flow, neglect of approach shear) since the numerical model handles the latter correctly.

Given that the fractional velocity reduction at small k_r is of order k_r, it is necessary to correct a formula given by Wilson (1985) which is wrong for small k_r. A formula for the fractional velocity reduction in the near lee of a porous windbreak which is satisfactory in this respect (and gives an equally good summary of the simulation experiments from which the original formula was derived) is

$$\frac{\Delta\bar{u}}{\bar{u}_o} = -\frac{k_r}{(1+2k_r)^{0{\cdot}8}}. \tag{35}$$

In conclusion, although our solution is an improvement upon earlier analytical treatments of porous-barrier flow, we admit that it has little but 'curiosity' value, because of the oversimplifications we have introduced (extreme porosity, homogeneous turbulence, neglect of approach shear, imposed eddy viscosity). We do however hope that our attempt may encourage the search for a more realistic analytical solution for windbreak flow.

APPENDIX
Terminology and Notation

Symbols

F_D	Force exerted by the flow on given area of the barrier
H	Barrier height
k	Turbulent kinetic energy per unit mass, or wavenumber.
k_r	Pressure loss (resistance) coefficient.
k_v	Von Karman's constant (=0·4)
K	Eddy viscosity
L	Arbitrary (large) dimensionless height at which upper boundary condition is imposed for analytical solution for streamfunction
m,n	Exponents in power-law profile for (respectively) the mean streamwise velocity and the eddy viscosity
p	Pressure
p	Dimensionless pressure $\bar{p}/\rho\bar{u}_{oH}^2$
R	Reynolds number, $u_{oH}H/K_H$
$s(z_1,z_2)$	Dimensionless unit-step function, zero for $z_1 > z_2$
t	Time
u,v,w	Streamwise (x), horizontal cross-stream (y), and vertical (z) velocity components
$\Delta\bar{u}$	Change in the mean streamwise velocity ($\bar{u} = \bar{u}_o + \Delta u$)
$\Delta\bar{w}$	Change in the mean vertical velocity ($\bar{w} = \Delta\bar{w}$)
u',v',w'	Fluctuating velocities, $u(t) = \bar{u} + u'(t)$, etc.
u, w	Dimensionless velocities; $u = \bar{u}/\bar{u}_{oH}$, $w = \bar{w}/\bar{u}_{oH}$
u_*	Friction velocity
x,y,z	Streamwise, horizontal cross-stream, and vertical coordinates. Used both as dimensional coordinates and as non-dimensional coordinates scaled on barrier height H.
$X^n(x)$	Function appearing in series solution for the perturbation streamfunction
z_o	Surface roughness length
δ	Boundary layer depth
$\delta(x_1,x_2)$	Delta function on x-coordinate
ε	Rate of dissipation of turbulent kinetic energy
ρ	Density
ν	Kinematic viscosity
Ω	Vorticity
Φ	Stream-function
ϕ_o, $\phi^{(1)}$, $\phi^{(2)}$	Terms in perturbation expansion of stream-function in k_r, appearing at indicated order
σ	Empirical parameter appearing in mixing-layer solution.

Overbar notation

An overbar denotes an average value, a tilde the Fourier transform along the x-coordinate.

Subscript notation

o	denotes unperturbed (far upstream) value
H	denotes value at $z = H$

Superscript notation

(a)	component of expansion in k_r alone; appears at order $(k_r)^a$
$(a)(b)$	component of expansion in k_r, m, $(1/R)$; appears at order $(k_r)^a(m)^b(1/R)^0$

Example: $\mathbf{u} = \overline{u}/\overline{u}_{oH} = \mathbf{u}_o + k_r\mathbf{u}^{(1)} + k_r^2\mathbf{u}^{(2)} + \ldots$
To first order in k_r, then
$\overline{u} = \overline{u}_o + \Delta\overline{u} = \overline{u}_o + k_r u_{oH}\mathbf{u}^{(1)}$
$\Delta\overline{u}/\overline{u}_{oH} = k_r\mathbf{u}^{(1)}$

Acknowledgements

The authors would like to thank Dr. J. J. Finnigan and an anonymous reviewer for their patient and constructive review of the first draft of this paper. This research has been supported by the Natural Sciences and Engineering Research Council of Canada.

References

Baines, W. D. and Peterson, E. G. 1951 An investigation of flow through screens. *Trans. ASME* **73,** 467–480

Batchelor, G. K. 1985 *An introduction to fluid dynamics*, Cambridge University Press

Bradley, E. F. and Mulhearn, P. J. 1983 Development of velocity and shear stress distributions in the wake of a porous shelter fence, *J. Wind Eng. Ind. Aerodyn.*, **15,** 157–168

Bradshaw, P. 1973 Effects of streamline curvature on turbulent flow. P. 7, AGARDOGRAPH #169, Ed. A. D. Young, Nat. Tech. Info. Service, U.S. Dept. Commerce

Churchill, R. V., Brown, J. W. and Verhey, R. F. 1974 *Complex variables and applications*, 3rd ed. McGraw-Hill

Counihan, J., Hunt, J. C. R. and Jackson, P. S. 1974 Wakes behind two-dimensional surface obstacles in turbulent boundary-layers, *J. Fluid Mech.*, **64,** 529–563

De Bray, B. G. 1971 Protection by fences. *Proceedings seminar on wind effects on buildings and structures*. Univ. of Auckland, May 1971

Durst, F. and Rastogi, A. K. 1980 Turbulent flow over two-dimensional fences. Pp. 218–232 of *Turbulent shear flows*, Vol. **2,** selected papers from the *2nd Int. symposium on turbulent shear flows, London, 1979*. Springer-Verlag, Berlin

Finnigan, J. J. 1985 Turbulent transport in flexible plant canopies, *The forest-atmosphere interaction*. Eds. B. A. Hutchison and B. B. Hicks, D. Reidel Pub. Co.

Graham, J. M. R. 1976 Turbulent flow past a porous plate, *J. Fluid Mech.*, **73,** 565–591

Hagen, L. J., Skidmore, E. L., Miller, P. L. and Kipp, J. E. 1981 Simulation of effect of wind barriers on airflows, *Trans. ASAE*, **24,** 1002–1008

Heisler, G. M. and DeWalle, D. R. 1988 'Effects of windbreak structure on wind flow', Chapter 2 of *Windbreak technology*, Eds. J. R. Brandle, D. L. Hintz and J. W. Sturrock. Elsevier. Also in *Agric. Ecosyst. Environ.*, **22/23**, 41–69

Kaiser, H. 1959 Die Strömung an Windschutzstreifen (The airflow through shelterbelts), Berichte Deutscher Wetterdienstes, Nr. 53. Band 7

Launder, B. E. and Spalding, D. B. 1974 The numerical computation of turbulent flows, *Comput. Methods Appl. Mech. Eng.*, **3,** 269–289

Laws, E. M. and Livesey, J. L. 1978 Flow through screens. *Ann. Rev. Fluid Mech.* **10,** 247–266

McNaughton, K. G. 1988 Effects of windbreaks on microclimate, Chapter 3 of *Windbreak technology*, Eds. J. R. Brandle, D. L. Hintz and J. W. Sturrock. Elsevier. Also in *Agric. Ecosyst. Environ.* **22/23**, 15–39

Plate, E. J. 1971 The aerodynamics of shelter belts, *Agr. Meteorol.*, **8,** 203–222

Raine, J. K. and Stevenson, D. C. 1977 Wind protection by model fences in a simulated atmospheric boundary layer, *J. Ind. Aerodyn.*, **2,** 159–180

Raupach, M. R. and Shaw, R. H. 1982 Averaging procedures for flow within vegetation canopies, *Boundary-Layer Meteorol.*, **22,** 79–90

Tani, N. 1958 On the wind tunnel test of the model shelter hedge, *Bull. Natl. Inst. Agric. Sci.*, Ser. A, No. 6, 75–80 (summary in English)

Taylor, G. I. 1944 'Air resistance of a flat plate of very porous material', Reports and Memoranda of the Aeronautical Research Council, No. 2236 (1944); reprinted (1963) No. 43, pp. 383–386 in *The scientific papers of G. I. Taylor, III*. Eds. G. K. Batchelor, Cambridge University Press

Van Eimern, J., Karschon, R., Razumova, L. A. and Robertson, G. W. 1964 'Windbreaks and shelterbelts', W. M. O. Tech. Note, No. 59

Wilson, J. D. 1985 Numerical studies of flow through a windbreak, *J. Wind Eng. Ind. Aero.*, **21,** 119–154

Wilson, J. D. 1987 On the choice of a windbreak porosity profile, *Boundary-Layer Meteorol.*, **38,** 37–49

Wilson, N. R. and Shaw, R. H. 1977 A higher-order closure model for canopy flow, *J. Appl. Meteorol.*, **16,** 1197–1205